Asymmetry of the Pinning Force in Thin Nb Films in Parallel Magnetic Field

P. I. Bezotosny, S. Y. Gavrilkin,
A. N. Lykov, C. Attanasio, C. Cirillo &
S. L. Prischepa

Journal of Superconductivity and Novel Magnetism
Incorporating Novel Magnetism

ISSN 1557-1939
Volume 24
Number 5

J Supercond Nov Magn (2011)
24:1553-1557
DOI 10.1007/
s10948-010-1053-9

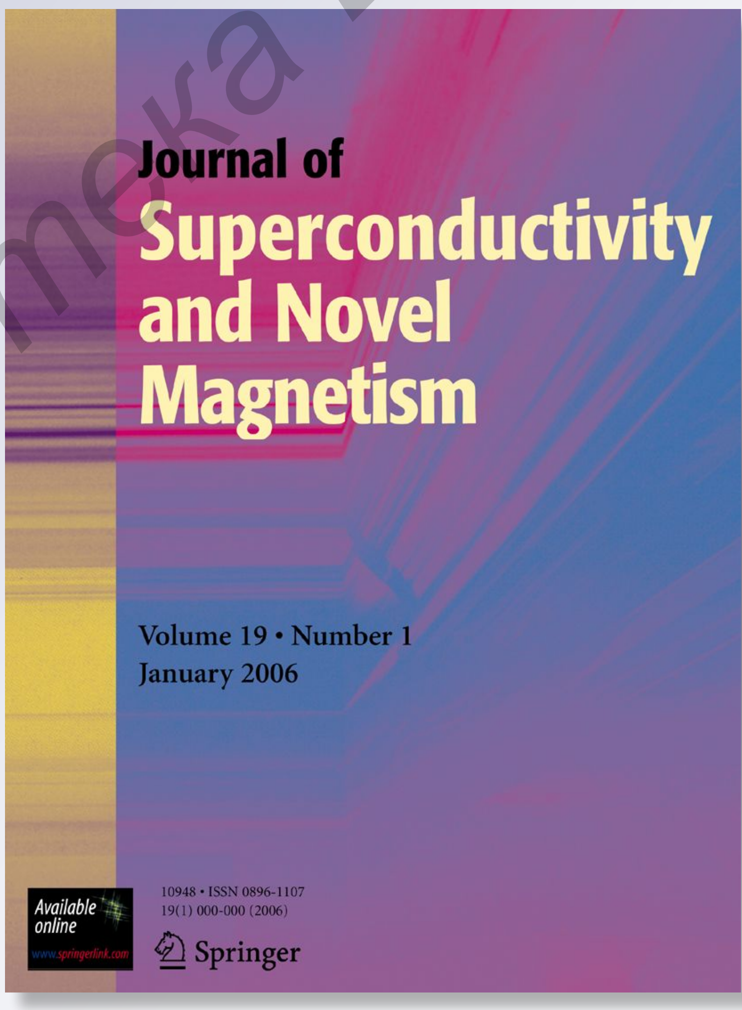

Библиотека БГУИР

Springer

Your article is protected by copyright and all rights are held exclusively by Springer Science+Business Media, LLC. This e-offprint is for personal use only and shall not be self-archived in electronic repositories. If you wish to self-archive your work, please use the accepted author's version for posting to your own website or your institution's repository. You may further deposit the accepted author's version on a funder's repository at a funder's request, provided it is not made publicly available until 12 months after publication.

Библиотека БГУИР

Author's personal copy

J Supercond Nov Magn (2011) 24:1553–1557
DOI 10.1007/s10948-010-1053-9

Asymmetry of the Pinning Force in Thin Nb Films in Parallel Magnetic Field

P.I. Bezotosny · S.Y. Gavrilkin · A.N. Lykov · C. Attanasio · C. Cirillo · S.L. Prischepa

Received: 20 April 2010 / Accepted: 6 October 2010 / Published online: 27 October 2010
© Springer Science+Business Media, LLC 2010

Abstract The pinning force, F_p, is studied in Nb films of different thickness in parallel magnetic field H. The asymmetry in the magnetic field dependence of F_p has been observed for two opposite directions of the transport current. The effect is less pronounced for thin and thick films where, respectively, single vortex pinning and pinning of the internal vortices, is relevant. At intermediate thickness, where the pinning mechanism is mostly caused by surface effects, an asymmetry in the $F_p(H)$ dependence is clearly visible. The different surface barriers that vortices should overcome to enter the sample from opposite sides of the film explain the effect, as confirmed by numerical calculations. These have been obtained by solving the Ginzburg–Landau equations with asymmetric boundary conditions which take into account the different superconducting properties of the film–substrate and film–vacuum interface. Such difference can also explain the reduction of the critical current usually observed in thin films as a function of their thickness.

Keywords Superconducting film · Asymmetry · Critical current · Boundary conditions

P.I. Bezotosny · S.Y. Gavrilkin · A.N. Lykov (✉)
P.N. Lebedev Physical Institute RAS, Leninsky Prospekt 53, 119991 Moscow, Russia
e-mail: lykov@lebedev.ru

C. Attanasio · C. Cirillo
CNR-SPIN Salerno and Dipartimento di Fisica "E. R. Caianiello", Università degli Studi di Salerno, Fisciano (Sa) 84084, Italy

S.L. Prischepa
Belarus State University of Informatics and RadioElectronics, P. Browka Street 6, Minsk 220013, Belarus

1 Introduction

In bulk superconductors the critical current I_c is determined by the interaction (pinning) of the vortex lattice with defects. In superconducting thin films it has been demonstrated that also the film thickness d plays a role in determining the critical current density, J_c [1–3]. For example, it has been shown that for parallel orientation of the external magnetic field, a crossover from collective to individual pinning occurs when d is lowered [2]. In this case, if $d < \lambda$ (where λ is the magnetic field penetration depth), the vortex lattice becomes less elastic in parallel magnetic field and J_c grows when d decreases [2]. If the microstructure of the sample is neglected, the vortex-free Meissner state should appear in a wide range of magnetic fields and J_c will be determined by the depairing current density, J_{dp}. However, the inhomogeneities of the film reduce the J_c values which decrease when d becomes smaller [3]. In general, the transition from the Meissner to the mixed state in thin films starts with the penetration of a single vortex chain. If the magnetic field is increased, the number of vortices in the chain grows up and, at some value, the chain splits. Further increase of the field causes the split of three chains, and so on. The position of the vortex chains is determined by the interaction with the free surfaces of the film. When the distances between vortex chains are commensurate with d, maxima in $J_c(H)$ dependence are present [3–10].

Vortex pinning mechanisms have been usually analyzed on the basis of the Ginzburg–Landau (G–L) theory [11] in which, as is well known, boundary conditions play a very important role [12]. If a superconducting sheet is in contact with the vacuum, the boundary condition for the superconducting order parameter is usually written in the form

$$\partial\psi/\partial x|_{x=-d/2,d/2} = 0, \qquad (1)$$

Библиотека БГУИР

Author's personal copy

where ψ is the module of the order parameter. More general boundary conditions can be written in the form [12]

$$\partial\psi/\partial x|_{x=-d/2,d/2} = \pm\psi/\Lambda, \quad (2)$$

where Λ is a phenomenological coefficient. Equation (2) is a very common condition which gives zero for the component of the current density normal to the boundary. In Ref. [13] it was shown that Λ depends on the properties of the material the superconductor is in contact with. In particular, if the superconductor is in contact with an insulating material, $\Lambda = \infty$ and boundary conditions (1) are valid. In the case of a superconductor-normal metal boundary, Λ is of the order of hundreds of nm [14].

From the G–L theory an approximate expression follows: $\Lambda \approx \frac{\xi^2(0)T_c}{a(T_c - T_{cs})}$ [15], where T_c is the superconducting critical temperature of the entire sample, T_{cs} is the superconducting critical temperature of the external layer (which is smaller than T_c due to degradation and to the proximity effect), a is the lattice constant and $\xi(0)$ is the zero-temperature G–L coherence length. Taking from Ref. [3] $\xi(0) = 7.4$ nm, $T_c = 7.5$ K, then $a = 0.33$ nm [16] and assuming $T_c/(T - T_{cs}) \sim T_c$, we get $\Lambda \sim 100$–200 nm for the Nb films which will be analyzed in this work. It has been shown that boundary conditions (2) lead to a depression of the order parameter [13, 15], and they were used to explain the decrease of T_c observed in thin Pb, Nb and Bi superconducting films [14]. It is also clear that the numerical values for Λ should be different on the two boundaries of the film because it interacts with the substrate on one side and with the vacuum on the other. This results in different conditions for the vortices to enter the sample, which can produce an asymmetry of J_c for opposite polarities of the transport current and/or magnetic field.

To check this idea and the applicability of the boundary conditions (2) to the G–L equations, a study of the pinning mechanisms has been systematically performed in Nb superconducting films of different thickness. The distinctive feature of our work is the study of the vortex motion in two directions: toward the substrate and toward the free surface of the sample. This condition has been obtained in the experiment by changing the direction of the transport current which was always applied parallel to the sample surface and perpendicular to the external magnetic field H (in turn applied in the direction parallel to the plane of the films). The detailed description of the experimental setup is published elsewhere [17]. The paper is organized as follows. In Sect. 2 we describe the preparation and characterization of the samples. In Sect. 3 we discuss the results obtained on Nb films. In Sect. 4 the main results of the paper are presented: the model and the numerical calculations.

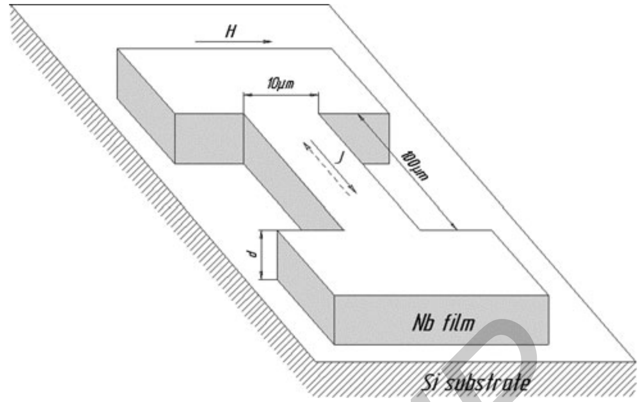

Fig. 1 Sketch of the measurement arrangement

2 Experimental

Nb films were grown on Si(100) substrates by dc sputtering. The thickness of the films was varied in the range between 16 and 103 nm. A standard lift-off technique was used to define the geometry of the samples which consists of stripes 10 μm wide and 90 μm long. The X-ray analysis of the samples revealed that the Nb films are granular with grain dimensions of the order of 10 nm and that a surface roughness of the order of few nanometers is present on the samples. More details about the structural characterization of the Nb films can be found elsewhere [3].

Current–voltage characteristics were measured using the standard four-point technique. I_c was determined as the transport current at which the voltage drop on the sample is equal to 1 μV. The detection of the critical current in our experiment was fully automated and this allowed us to determine the voltage drop with an accuracy of 0.1 μV. All the measurements were performed in liquid helium at $T = 4.2$ K with samples fully immersed in the bath. Figure 1 shows a sketch of the measurement method used in our experiments. The distinctive feature of our work is the change of the polarity of the transport current (which we call positive or negative), which was applied always parallel to the film's surface and perpendicular to the applied magnetic field which was directed parallel to the film's surface.

3 Results ob Nb Films of Different Thickness

$J_c(H)$ have been measured for two opposite directions of the bias current: we call them J_c^+ and J_c^-. The results for the dependence of the corresponding pinning forces on the applied magnetic field, $F_p^+(H) = \mu_0 J_c^+ H$ and $F_p^-(H) = \mu_0 J_c^- H$, for the sample with $d = 32$ nm are shown in Fig. 2. It can be seen that the two curves are very similar even if some spread of the data is present for $\mu_0 H > 0.6$ T. As it was shown in Ref. [3], the single vortex pinning is the predominant pinning mechanism for Nb films with thickness in

Библиотека БГУИР

Author's personal copy

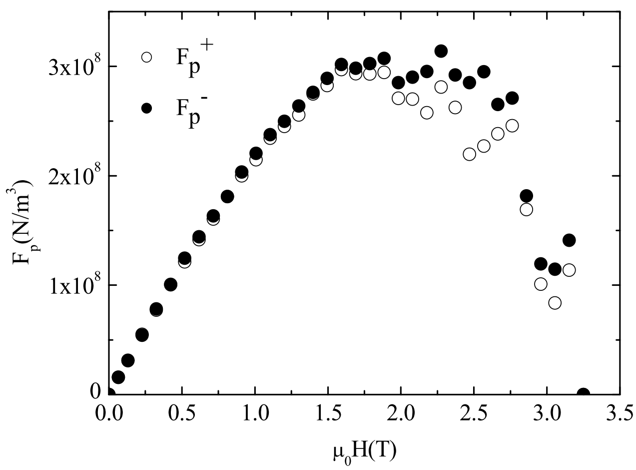

Fig. 2 Magnetic field dependence of the pinning force for the two directions of the bias current for the Nb thin film with $d = 32$ nm. *Open* (*closed*) *circles* refer to F_p^+ (F_p^-)

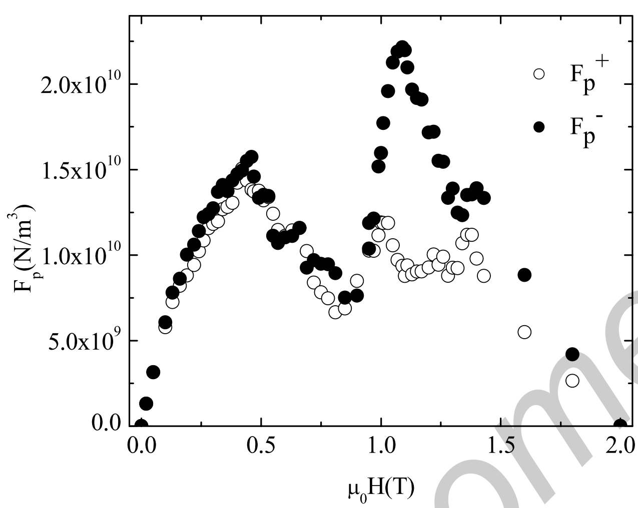

Fig. 3 Magnetic field dependence of the pinning force for the two directions of the bias current for the Nb thin film with $d = 81.5$ nm. *Open* (*closed*) *circles* refer to F_p^+ (F_p^-)

the range 16–32 nm (see Fig. 8b of Ref. [3]) and the role of the boundaries is not relevant in this case.

The situation is completely different for the sample with $d = 81.5$ nm. The results for the $F_p^{\pm}(H)$ measurements are shown in Fig. 3. At $\mu_0 H \approx 1.1$ T a sharp increase of F_p^+ is present while a plateau-like behavior is obtained for F_p^-. In Ref. [3] we have shown that the peak in the $F_p(H)$ dependence is related to commensurability effects because for thicker samples the vertical dimension of the samples begins to play an important role and maxima, which correspond to the commensurability between the film thickness and the vortex spacing, are observed [3]. In this case, the commensurability field ($\mu_0 H = 1.1$ T) corresponds to the average vortex spacing $a_0 \sim (\Phi_0/\mu_0 H)^{1/2} \sim 43$ nm which is very close to half of the film thickness. This effect on

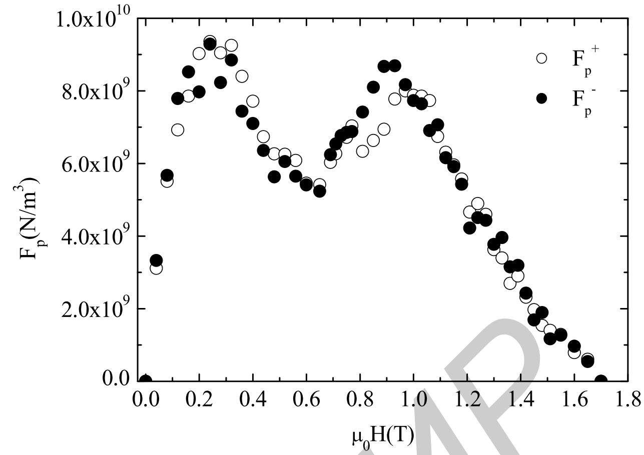

Fig. 4 Magnetic field dependence of the pinning force for the two directions of the bias current for the Nb thin film with $d = 101.3$ nm. *Open* (*closed*) *circles* refer to F_p^+ (F_p^-)

thick vanadium films was already observed by Fogel and Cherkasova [7]. In addition, the large difference observed between F_p^+ and F_p^- in the region close to the commensurability field corresponds to the different energy barriers that vortices should overcome in order to enter the sample. In one case, the surface barrier is determined by the Nb/Si interface and in the case of the opposite vortex motions, it is determined by the free Nb surface. For the thicker Nb film ($d = 103.1$ nm) we get again a commensurability effect, but at $\mu_0 H = 0.9$ T, which corresponds to the average vortex spacing $a_0 \approx 50$ nm, i.e. half of the film thickness, see Fig. 4. However, in this case, the two curves for $F_p^+(H)$ and $F_p^-(H)$ are very similar, because for larger values of d the weight of the interface on the superconducting properties becomes less relevant.

4 The Model and the Results of Numerical Calculations

In order to interpret our experimental results, we considered, for the sake of simplicity, the case in which no vortices flow in the superconductor. This theoretical approach, even if simplified, can explain our data. Let us consider a long and wide superconducting plate of thickness d in a magnetic field. The field is assumed to be parallel to the plate surface. A transport current I_t flowing through the plate is also parallel to its surface and perpendicular to the external field. The system of the G–L equations has the form [3]

$$\frac{4\pi}{c}\mathbf{j}_s = \frac{\psi^2}{\lambda^2}\left(\frac{\phi_0}{2\pi}\nabla\theta - \mathbf{A}\right), \tag{3}$$

$$\nabla^2\psi - \left(\nabla\theta - \frac{2\pi}{\phi_0}\mathbf{A}\right)^2\psi + \frac{1}{\xi^2}(\psi - \psi^3) = 0, \tag{4}$$

Библиотека БГУИР

Author's personal copy

where $\mathbf{A}$ is the vector potential of the magnetic field ($\mathbf{B} = \operatorname{rot}\mathbf{A}$) and $\mathbf{j}_s$ is the current density in the superconductor. In accordance with Maxwell equation,

$$\operatorname{rot}\operatorname{rot}\mathbf{A} = \frac{4\pi}{c}\mathbf{j}_s. \tag{5}$$

In general, the order parameter is written in the form $\Psi = \psi e^{i\theta}$, where θ is the phase of the order parameter. Let us consider a Cartesian coordinate system (x, y, z). Let y and z axes lay in the plane of the plate surface (z is directed along the external magnetic field H). Then, the vector potential has only y component: $\mathbf{A} = \mathbf{e}_y A(x)$. Since the transport current flowing per unit of the plate width I_t induces a magnetic field $H_I = 2\pi I_t/c$ on its surface, the total field near the plate surfaces is $H \pm H_I$. It defines the boundary conditions for the magnetic field.

In contrast to our previous work [3] in which the usual boundary conditions (1) for the superconducting order parameter were used, in this work we apply the general boundary conditions on the two surfaces in the form

$$\partial\psi/\partial x = \frac{\psi}{\Lambda_1}\bigg|_{x=-d/2}, \tag{6a}$$

$$\partial\psi/\partial x = -\frac{\psi}{\Lambda_2}\bigg|_{x=d/2}, \tag{6b}$$

where Λ_1 and Λ_2 are phenomenological coefficients. The critical current is determined by the maximum transport current at which a solution of the G–L equations can be found. Thus the solution is absent in the vortex-free case if $J > J_c$ and for thick films, vortices begin to penetrate into the film. In this case it is possible to say that the critical current is determined by the appearance of vortices in the superconducting plates and the only pinning centers are the boundaries of the plates.

The theoretical dependence of the pinning force on the applied magnetic field was obtained using the samples' parameters as experimentally determined. In Figs. 5 and 6, the calculated dependence of $\mu_0 J_c H$ (which is analogous to the pinning force F_p) as a function of H is reported as examples, using the parameters for the samples with $d = 81.5$ nm and $d = 32$ nm reported in Ref. [3]. To take into account the different properties of the boundaries, we chose $\Lambda_1 = 140$ nm and $\Lambda_2 = 70$ nm. A similar value for the phenomenological parameter Λ was used in Ref. [14] to explain the $T_c(d)$ dependence observed in Nb films. The theoretical curves in Fig. 5 reproduce the asymmetry of the magnetic field dependence for F_p^+ and F_p^- as it was experimentally observed when the direction of the bias current was inverted, while the two curves in Fig. 6 are very similar. So in agreement with experiments, the asymmetry of the calculated dependence of $\mu_0 J_c H$ on H for thin film ($d = 32$ nm) is smaller than the one derived for the film with $d = 81.5$ nm. The results confirm that the asymmetry observed in our experiments is due

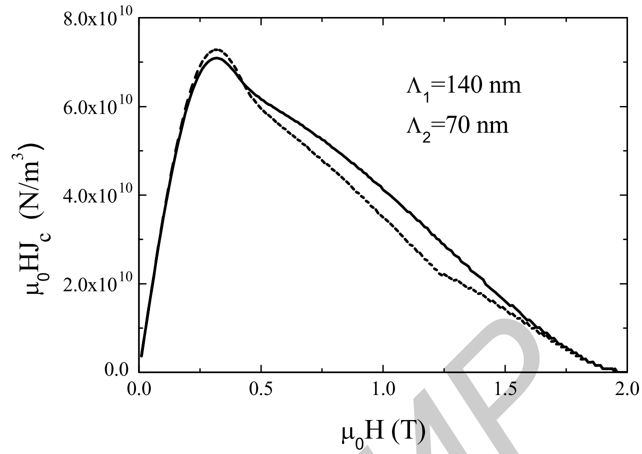

Fig. 5 The calculated dependence of $\mu_0 J_c H$ versus the parallel magnetic field for the forward (*solid line*) and backward (*dashed line*) direction of the transport current for the film with $d = 81.5$ nm. For details about the parameters Λ_1 and Λ_2 given in the figure, see the text

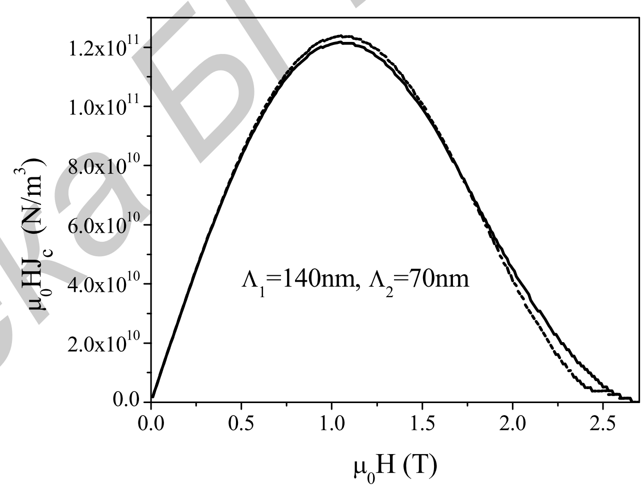

Fig. 6 The calculated dependence of $\mu_0 J_c H$ versus the parallel magnetic field for the forward (*solid line*) and backward (*dashed line*) direction of the transport current for the film with $d = 32$ nm

to the different conditions in which the vortices act when entering the film respectively from the substrate or from the outer boundary. We assumed in our calculations that the disappearance of the vortex-free state leads to a resistive state. It should be noted that the vortex-free model does not work in the case of thick films in strong magnetic field when H is close to the upper critical field of the film H_{c2}, because vortices begin to penetrate into the film. Also, the calculated $\mu_0 J_c H$ curves do not show the presence of the two maxima in the case of thicker samples, which are observed in the experiment (see Figs. 2 and 3). This is due to the different nature of the $F_p(H)$ and $\mu_0 J_c H$ curves in the two cases. In fact, in the free vortex limit the order parameter is suppressed only at the surface of the film and the vortices are absent in the sample. In our experiment, vortices are present

Библиотека БГУИР

Author's personal copy

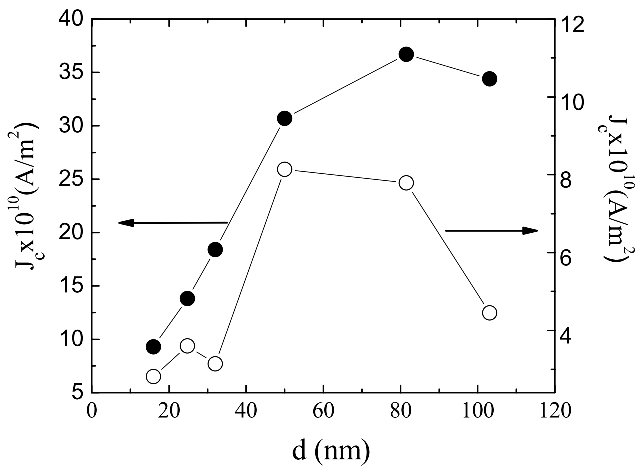

Fig. 7 The experimental (theoretical) $J_c(d)$ dependence is shown by *open* (*closed*) *symbols*. $\Lambda_1 = 140$ nm, $\Lambda_2 = 70$ nm were used in the numerical simulation. For further details on the parameters used in the simulation, see the text

in the thick films at high fields where critical current is also due to pinning of the vortex lattice. As a result, when the period of the vortex structure is equal to the film thickness, another local maximum in the $F_p(H)$ is present [3].

There is a second experimental result which can be explained using this approach, namely the decrease of J_c when the thickness of the superconducting films becomes smaller [3]. The experimental $J_c(d)$ dependence obtained on our samples at zero magnetic field and $T = 4.2$ K is shown on Fig. 7 (lower curve). If boundary conditions (1) are used, the G–L equations give $J_c(d) \to J_{dp}$ when $d \to 0$. On the other hand, boundary conditions (6a) and (6b) lead to the suppression of the superconducting order parameter at the edges of the plate and, as a result, to the decrease of J_c. Figure 7 shows also the calculated $J_c(d)$ dependence at $T = 4.2$ K and $H = 0$ (upper curve). Again here we used the experimental parameters for the niobium films reported in Ref. [3] and $\Lambda_1 = 140$ nm and $\Lambda_2 = 70$ nm. In agreement with the experiment, for $d < 50$ nm, J_c decreases with decreasing thickness of the film. In this approach the decrease of J_c is due to the influence of the boundary conditions (2) whose role is stronger when the thickness of the superconducting film becomes smaller.

However, two results obtained in experiments are not reproduced by the proposed theoretical model. First, the values of the calculated critical current and pinning force are significantly higher compared to the experimental ones. This could be related to the highly granular structure of our niobium films [3]. Grain boundaries act as weak links and significantly reduce J_c of the film. In this respect, the theoretical dependence for $F_p(H)$ and $J_c(d)$ can be interpreted as an upper limit for both these quantities in parallel field. The second point missing in the theoretical picture is the presence of the two maxima in the thicker films. This is due to the assumption that no vortices are present when the magnetic field is applied to the sample. However, as already underlined above, in experiments the vortices are present in the samples and J_c is also due to their pinning with defects. So, when the period of the vortex lattice is equal to d, another local maximum in the $F_p(H)$ dependence is present as observed in the experiment.

5 Conclusions

In conclusion, pinning properties of Nb films with different thickness were investigated by measuring the $J_c(H)$ dependence for two opposite directions of the bias current in the presence of a parallel magnetic field. In a certain thickness range the critical current densities for opposite polarities of the bias current show a marked asymmetry. The vortex free case was theoretically analyzed on the basis of the G–L equations with asymmetric boundary conditions which reflect the fact that thin films have different interactions with the vacuum and the substrate. The reasonable agreement between the theory and the experimental data confirms the validity of the model.

Acknowledgements The authors are grateful to A.Yu. Tsvetkov for help in the work. This work was in part financially supported by the Program of Russian Academy of Sciences No. 27.

References

1. Wördenweber, R.W., Kes, P.H.: Phys. Rev. B **34**, 494 (1986)
2. Stejic, G., Gurevich, A., Kadyrov, E., Christen, D., Joynt, R., Larbalestier, D.C.: Phys. Rev. B **49**, 1274 (1994)
3. Prischepa, S.L., Montemurro, D., Cirillo, C., Attanasio, C., Salvato, M., Merlo, V., Lykov, A.N., Tsvetkov, A.Yu.: Supercond. Sci. Technol. **19**, 1124 (2006)
4. Sutton, J.: Proc. Phys. Soc. **67**, 791 (1966)
5. Yamashita, T., Onodera, Y.: Solid State Commun. **13**, 1289 (1973)
6. Yamashita, T., Rinderer, I.: J. Low Temp. Phys. **24**, 695 (1976)
7. Fogel, N.Ya., Cherkasova, V.G.: Physica B **107**, 291 (1981)
8. Ichkitadze, L.P., Skobelkin, V.I.: Fiz. Nizk. Temp. **7**, 117 (1981). Sov. J. Low Temp. Phys. **7**, 58 (1981)
9. Ziese, M., Esquinazi, P., Wagner, P., Adrian, H., Brongersma, S.H., Griessen, R.: Phys. Rev. B **53**, 8658 (1996)
10. Fogel, N.Ya., Buchstab, E.I., Cherkasova, V.G., Yuzephovich, O.I., Mikhailov, M.Yu., Stezenko, A.N.: Low Temp. Phys. **27**, 752 (2001)
11. Blatter, G., Feigel'man, M.V., Geshkenbein, V.B., Larkin, A.I., Vinokur, V.M.: Rev. Mod. Phys. **66**, 1125 (1994)
12. De Gennes, P.G.: Rev. Mod. Phys. **36**, 225 (1964)
13. Zaitsev, R.O.: Zh. Eksp. Teor. Fiz. **48**, 1759 (1965)
14. Simonin, J.: Phys. Rev. B **33**, 7830 (1986)
15. Andrushin, E.A., Ginzburg, V.L., Silin, A.P.: Sov. Phys. Usp. **163**, 105 (1993)
16. Kittel, C.: Introduction to Solid State Physics Wiley, New York (1996)
17. Gavrilkin, S.Yu., Ivanenko, O.M., Lykov, A.N., Mitsen, K.V., Tsvetkov, A.Yu., Attanasio, C., Cirillo, C., Prischepa, S.L.: Supercond. Sci. Technol. **23**, 065019 (2010)

Библиотека БГУИР